ASTRONOMY & ASTROPHYSICS
SUPPLEMENT SERIES

Astron. Astrophys. Suppl. Ser. **129,** 609-615 (1998)

Removing the photon-centroiding hole in optical stellar interferometry

P. Berio, F. Vakili, D. Mourard, and D. Bonneau

Observatoire de la Côte d'Azur, Département Fresnel, CNRS UMR 6528, 06460 Saint Vallier de Thiey, France

Received April 7; accepted October 24, 1997

Abstract. We describe a technique to remove the photon-centroiding hole from event-sensitive intensified cameras. This effect degrades the average power-spectrum of short-exposures and can bias the fringe visibility estimates from a long baseline stellar interferometer. Using a simple numerical model and 2D interpolating techniques we show that this hole can be corrected directly from actual interferograms on the object itself. We apply our technique to stars with different visual magnitudes, i.e. different photon rates, which have been observed by the GI2T interferometer. The proposed method can significantly improve the GI2T observations providing robust estimates of visibilities whatever the photon rate in clipped short exposures.

Key words: techniques: interferometric — methods: data analysis — instrumentation: detectors

1. Introduction

Since Labeyrie's invention of stellar speckle-interferometry (Labeyrie 1970; Dainty 1975), high angular resolution techniques have been able to attain the diffraction limit of existing large telescopes both in the visible and infra-red wavelengths. Using the more recent technique of speckle-imaging like the bi-spectral analysis (Weigelt 1977), one can have access to the morphological structures of various galactic and extra-galactic objects such as T Tauri stars or NGC 1068 (Thiébaut et al. 1995; Weigelt 1977). A practical problem often encountered in reducing speckle-interferometric data is the so-called "photon-centroiding hole" (Foy 1987), PCH hereafter, which degrades the power spectra or bi-spectra of short exposures recorded by intensified cameras (Thiébaut et al. 1995). This hole is due to the spatial/temporal coincidence of photon-events and appears as a depression at the center of the average auto-correlation, AC hereafter, of clipped speckle-interferograms. Consequently, the observed Fourier components are biased at different spatial frequencies and make the restored AC or reconstructed image of the object unreliable. Different remedies have been proposed to overcome this problem such as calibrating it on a laboratory source having photometric properties close to those of the star under study or by comparing the raw power spectra to a priori models from which the hole can be removed (Hoffman 1993). A different but most effective technique consists in spatially splitting the speckle-interferograms in two optical replicas which are later cross-correlated by software (Thiébaut 1994). If these replicas are strictly balanced, the cross-correlation, CC hereafter, is identical to the AC with the extra bonus of obtaining an unbiased power-spectrum after Fourier transformation. The counterpart is doubling the number of pixels on the detector and penalizing the signal to noise ratio by a factor $\sqrt{2}$.

In this paper we propose a different approach which consists in correcting the artifact of the PCH directly from the power-spectrum itself provided a partial coverage of the Fourier space due to a sparse pupil distribution. This is precisely the case of a diluted optical interferometer such as the GI2T (Grand Interféromètre à 2 Télescopes), where the power-spectrum support is limited to one low frequency component and two high-frequency symmetrical components with respect to the zero frequency.

In the first section we recall briefly the instrumental characteristics of the GI2T and its detector relevant to this study. We describe also the proposed technique to overcome the PCH. In the second section, we present the theoretical expressions of the standard deviation of the power and cross-power spectra, which are used to estimate the quality of the PCH correction. Next we present the correction results on numerical simulated interferograms. Our method is then applied to data from actual observations on the sky where reliable visibilities have been obtained for two stars with different magnitudes. Finally we discuss the limitation of our method and its use on future interferometers.

2. Observing in the photon-starved regime with the GI2T

2.1. The CP40 detector and data-collection

The GI2T has been described in two recent papers (Mourard et al. 1994a; Mourard et al. 1994b, M94b hereafter). In stellar interferometry, the multi-dimensional coherence volume of the incoming wavefront must be correctly sampled in order to maximize the signal to noise ratio of high angular resolution collected data. GI2T uses two 1.5 m primary mirrors much larger than the r_0 Fried's parameter in the visible (Fried 1965) characterizing the spatial coherence area. In practice, the light beams from GI2T's telescopes are recombined in an image plane after output pupil remapping. The multi-speckle interferograms feed a spectrograph whose entrance slit is one speckle wide and about 10 speckles high. A high magnification of these interferograms on the focal detector is done in order to correctly sample the interference fringes. In addition, the exposure time of the detector must be short enough to correctly sample the temporal variation of the atmospheric turbulence, i.e. its coherence time. Besides, the multi-r_0 operational mode of the GI2T results in an auxiliary dimension of the coherence volume related to the spectral correlation of the fringes as a function of wavelengths. This limits in practice the total bandwidth of the interferograms to a few nanometers (Berio et al. 1997). These overall constraints demand a fast detector with a large number of pixels. The CP40 camera (Blazit 1987) was built in the 1980's for the purpose of speckle and long-baseline interferometry with large apertures as for the GI2T. It is a 2-stage intensified photon-detector, with the output phosphorus screen coupled to a mosaic of 4 Thomson 288×384 CCD's which are readout at the standard TV rate of 20 ms. This camera is installed at the focal plane of the low-resolution spectrograph of the GI2T beam-combiner ($R \approx 4500$).

2.2. The PCH artifact

Among the problems that one may encounter with ICCD cameras, the PCH has dramatic consequences in the estimation of fringe visibility. For the GI2T (M94b), we estimate the visibility as the ratio of high frequency to low frequency energies in the average spectral density of short exposures. In practice, the first step of data processing consists in computing the average two-dimensional AC of these short exposures. The PCH appears at the center of the AC. The shape of this hole is not stationnary in time and depends strongly on the average number of photons per short exposure. Based upon data collected on more than 10 stars with different visual magnitudes, we have checked that the PCH converges to a 2D inverse gaussian function extending out to 3×3 points (Fig. 1) for large numbers of averaged AC. It is superimposed to the top of the fringe pattern which is symmetrized in the AC process. In a second step the power spectrum is obtained by Fourier transforming the AC. This transformation dilutes the PCH artifact over the whole spatial frequency domain where a large fraction of its energy extends beyond the cut-off frequency of the interference signal.

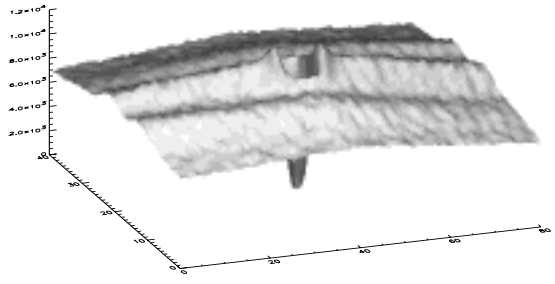

Fig. 1. The central part of the averaged AC of photon-noisy multi-speckle data recorded on α Cephei with the GI2T. The central depression corresponds to the PCH artifact

2.3. The PCH correction method

Our method aims at fitting a 2D polynomial function to the Fourier transform of the PCH in order to reconstruct the original unbiased power spectrum. Note that no assumption is made on the exact shape of the PCH Fourier transform. The fit uses the noise background, made of the photon noise and the PCH Fourier transform, over the large frequency domain beyond the fringe peak support. This is more efficient than in the direct space because the PCH has a narrow support at the center of the interferogram AC.

As already mentionned, the power spectrum of a diluted pupil such as the GI2T one includes 3 components: a low-frequency contribution (the sum of the AC of each aperture) and two symmetrical high-frequency components (the CC of apertures). The adopted correction method is based on masking these components, to fit a 2D polynomial distribution to the noise background and to substract it from the raw power spectrum, in order to obtain the original photon-unbiased power spectrum. As a by-product, one corrects also for the photon-bias in the averaged power spectrum.

In practice, the masked parts represent only a few percents of the power spectrum and besides we assume the continuity of the Fourier transform of the PCH, thus the fit interpolation in these parts is correct.

3. The standard deviation of the power spectrum

In practice, the GI2T dispersed fringes are processed following two methods: a) averaged AC of an interferogram spectral window ($\Delta\lambda$) for angular diameter determinations, b) averaged CC between two separate spectral windows of the interferograms ($\Delta\lambda_1$, $\Delta\lambda_2$) for the analysis of the stellar morphology as a function of Doppler shift across spectral lines (Fig. 2).

In this paragraph, we present theoretical expressions of the standard deviation of power and cross-power spectra. These spectra are computed by Fourier transforming the AC/CC of photon events in clipped images. The noise which affects these spectra comes from both the atmospheric turbulence (speckle noise) and photon noise. Roddier & Léna (1984) have given the variance of a photon unbiased estimate of the power spectrum as:

$$\sigma_{\rm p}^2 = N^4 \left\langle \left|\tilde{I}\right|^2 \right\rangle^2 + 2N^3 \left\langle \left|\tilde{I}\right|^2 \right\rangle + N^2, \quad (1)$$

where N is the average number of photons in the spectral channel and $\tilde{I}$ is the Fourier transform of the instantaneous irradiance distribution in the image.

Petrov (1986) has described the combined influence of atmospheric fluctuations and photon noise on the estimation of cross-power spectrum. The variance of this quantity is defined as:

$$\sigma_{\rm cp}^2 = N_1^2 N_2^2 \left\langle \left|\tilde{I}_1\right|^2 \left|\tilde{I}_2\right|^2 \right\rangle - N_1^2 N_2^2 \left|\left\langle \tilde{I}_1 \tilde{I}_2^* \right\rangle\right|^2 + N_1 N_2^2 \left\langle \left|\tilde{I}_2\right|^2 \right\rangle + N_1^2 N_2 \left\langle \left|\tilde{I}_1\right|^2 \right\rangle + N_1 N_2, \quad (2)$$

where N_1 and N_2 are the average photon number in each spectral channel and $\tilde{I}_1$ and $\tilde{I}_2$ are the Fourier transforms of the instantaneous irradiance distributions in these channels.

This can be applied to the real and imaginary part of the cross-power spectrum:

$$\sigma_{\rm RE(cp)}^2 = N_1^2 N_2^2 \left\langle \left|\tilde{I}_1\right|^2 \left|\tilde{I}_2\right|^2 \right\rangle - N_1^2 N_2^2 \left|\left\langle \tilde{I}_1 \tilde{I}_2^* \right\rangle\right|^2 + \frac{N_1 N_2^2}{2} \left\langle \left|\tilde{I}_2\right|^2 \right\rangle + \frac{N_1^2 N_2}{2} \left\langle \left|\tilde{I}_1\right|^2 \right\rangle + \frac{N_1 N_2}{2}, \quad (3)$$

$$\sigma_{\rm IM(cp)}^2 = \frac{N_1 N_2^2}{2} \left\langle \left|\tilde{I}_2\right|^2 \right\rangle + \frac{N_1^2 N_2}{2} \left\langle \left|\tilde{I}_1\right|^2 \right\rangle + \frac{N_1 N_2}{2}. \quad (4)$$

Note that in Eqs. (2) and (3), $< \tilde{I}_1 \tilde{I}_2^* >$ is a complex quantity.

4. Results

4.1. Application to photon-noisy simulated interferograms

Before applying our method to stellar interferograms obtained with the GI2T interferometer, we have evaluated its performances on simulated data from a numerical model for the GI2T+CP40. The model includes atmospheric disturbed wavefronts, photon-noise and the PCH effect itself following the operational mode of the GI2T described in Sect. 2.1.

In a first step, we produce phase disturbed wavefronts with a typical $D/r_0 = 10$ characteristic of good atmospheric conditions at the Calern Observatory. The wavefronts on the apertures are assumed uncorrelated (the baseline is larger than the outer scale). From each wavefront we produce the continuous distribution of intensity in the focal plane of the GI2T by computing the squared Fourier transform of the complex amplitude on the pupil. We have to produce these wavefronts at different wavelengths in order to simulate the spectrograph. We produce monochromatic interferograms at different wavelengths for a given state of turbulence. We select the central strip of these interferograms (one speckle wide) that we reassemble in increasing wavelengths in order to simulate the dispersed fringes over 100 Å ($\delta\lambda = 0.4$ Å). Next we generate the photon noise using this continuous distribution as the probability density of photon arrival on the detector. We average the AC of these short exposures for a typical number of 2000 different wavefront samples. We have chosen to simulate the PCH by substracting a narrow 2D gaussian from the center of the averaged AC. Thus by a Fourier transformation, we obtain a biased power spectrum, which is taken as the starting step for removing the PCH (Fig. 2). We emphasize that the choice of a gaussian is just to mimic a PCH effect in the AC. It does not influence the correction of the actual observations by GI2T on stellar sources.

Before the 2D polynomial fit of the noise background, we mask the low frequency and the two high frequency peaks, but also the horizontal and diagonal spikes introduced by the interferograms windowing (these spikes are shown in Figs. 2 and 3). The horizontal spike is due to the spectral windowing. The field windowing is done with an angle of 10 degrees which ensures that the fringe peaks are not contaminated by the associated spike. The width of the masks are fixed by the extent of low and high components in this spectrum.

In order to determine the polynomial degree for the best fit, we can make the following assumption based on the expected power spectrum. Knowing that the CC does not suffer from the PCH, it is possible to estimate the fit quality from the ratio $Q = \sigma_{\rm p}/\sigma_{\rm RE(cp)}$. We compute therefore the power spectrum and the cross-power spectrum corresponding respectively to the spectral band $\Delta\lambda$ and two spectral bands $\Delta\lambda_1$, $\Delta\lambda_2$. For a given image, $\sigma_{\rm p}$ and $\sigma_{\rm RE(cp)}$ are N and $\sqrt{N_1 N_2/2}$ respectively at high spatial frequencies. In order to compare the standard deviations of power and cross-power spectra, one must normalize $\sigma_{\rm p}$ by N^2 and $\sigma_{\rm RE(cp)}$ by $N_1 N_2$. Hence:

$$Q = \frac{\sqrt{2N_1 N_2}}{N}. \quad (5)$$

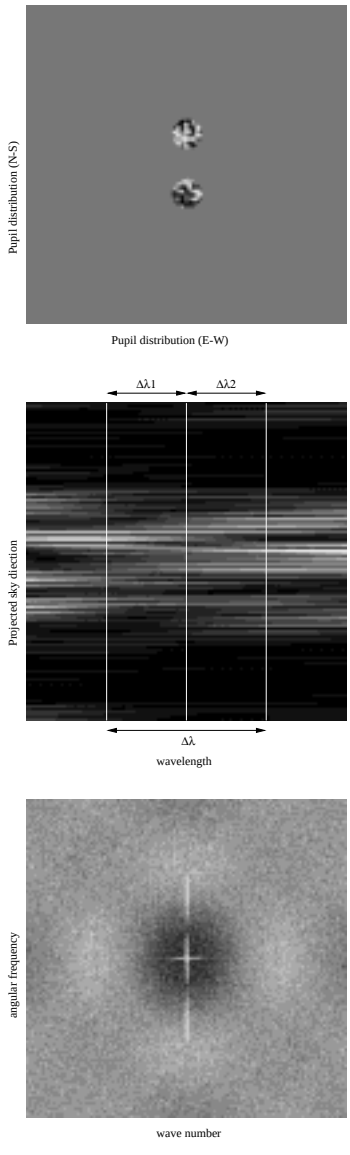

Fig. 2. Numerical simulation of the PCH. From the top to the bottom: typical phase disturbed wavefronts in the output-pupil plane of the GI2T, resulting dispersed fringes over 100 Å at the focal plane of the interferometer (the different spectral windows, used in the AC and CC computations, are presented), resulting power spectrum to which the PCH has been added

Now the best fit is obtained according to two criteria: the average noise background in the unbiased corrected power spectrum should be as close as possible to the theoretical zero value. Second the final ratio Q should approach the theoretical value fixed by N, N_1 and N_2. From Table 1, one can see that Q converges rapidly for increasing polynomial degrees. For instance, it stagnates at its theoretical value of 0.73 after the polynomial degree has reached 5.

Table 1. Correction quality versus polynomial degree. Photon-noisy simulated interferograms. $\sigma_{\rm noise}$ and $\mu_{\rm noise}$ are the standard deviation and the mean value of the photon noise in the power spectrum, expressed in fractions of the total energy. The theoretical ratio Q is 0.73 according to the number of photons in the different spectral windows

polynome degree	$\sigma_{\rm noise}$ $(\times 10^{-4})$	$\mu_{\rm noise}$ $(\times 10^{-7})$	Q
3	1.266	5.1	0.75
4	1.244	3.2	0.74
5	1.243	3.5	0.73
6	1.243	4.0	0.73
7	1.243	1.9	0.73

4.2. Application to stellar interferograms

The next step for validating our approach is to apply the method to actual interferometric data. As previously done on simulated spectra, we have analized the Q convergence versus polynomial degree. From Table 2, one can see that it stagnates at its predicted value of 0.77, fixed by the photon numbers in each spectral window of αCep interferograms, after the polynomial degree has reached 10. The need to iterate to high degrees comes from the fact that the PCH artifact appears actually as a more complex 2D distribution (Fig. 4). For instance, and depending on the average photon rate per pixel, it can exhibit positive "ears" (see Fig. 1 top) due to the CP40 centroiding hardware electronics. These "ears" create an additional modulation of spectral densities that high order polynomial fits completly eliminate (Fig. 3).

Figure 3 illustrates the results of our method applied to a bright star (α Cep, $V = 2.4$) and a faint star (P Cygni, $V = 4.8$).

Table 2. Correction quality versus polynomial degree. Observation of α Cephei on october 17th 1994. $\sigma_{\rm noise}$ and $\mu_{\rm noise}$ are the standard deviation and the mean value of the photon noise in the power spectrum, expressed in fractions of the total energy. The theoretical ratio Q is 0.77 according to the number of photons in the different spectral windows

polynome degree	$\sigma_{\rm noise}$ $(\times 10^{-5})$	$\mu_{\rm noise}$ $(\times 10^{-7})$	Q
5	4.431	18	1.10
6	3.659	4.0	0.92
7	3.648	4.0	0.91
8	3.229	9.5	0.81
9	3.225	7.4	0.80
10	3.108	2.7	0.78
11	3.107	4.4	0.77
12	3.107	3.8	0.77

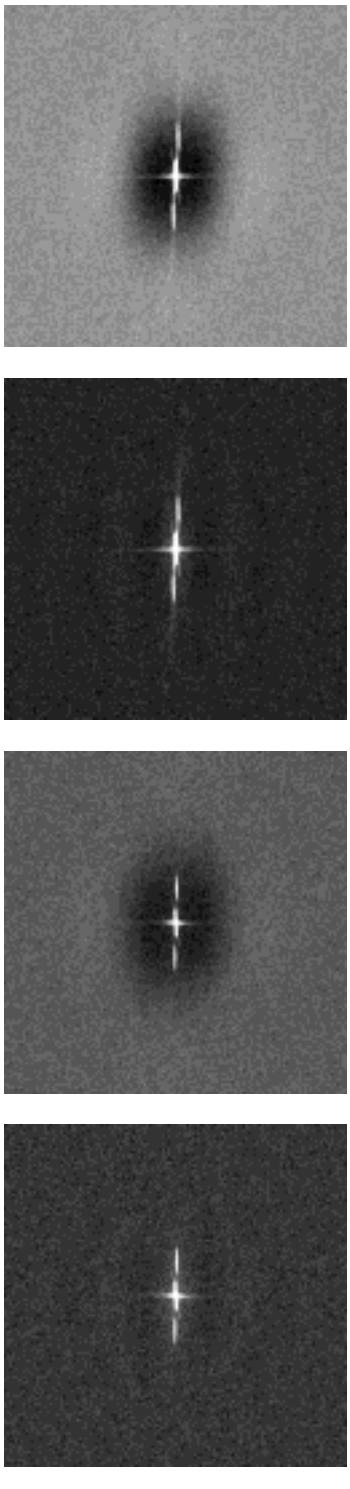

Fig. 3. Results of the correction technique on actual GI2T observations. The two top images display the biased and corrected power spectra of αCep. These at the bottom display PCyg. The polynomial degree is 11. The horizontal and vertical directions correspond respectively to the wave number and to the angular frequency

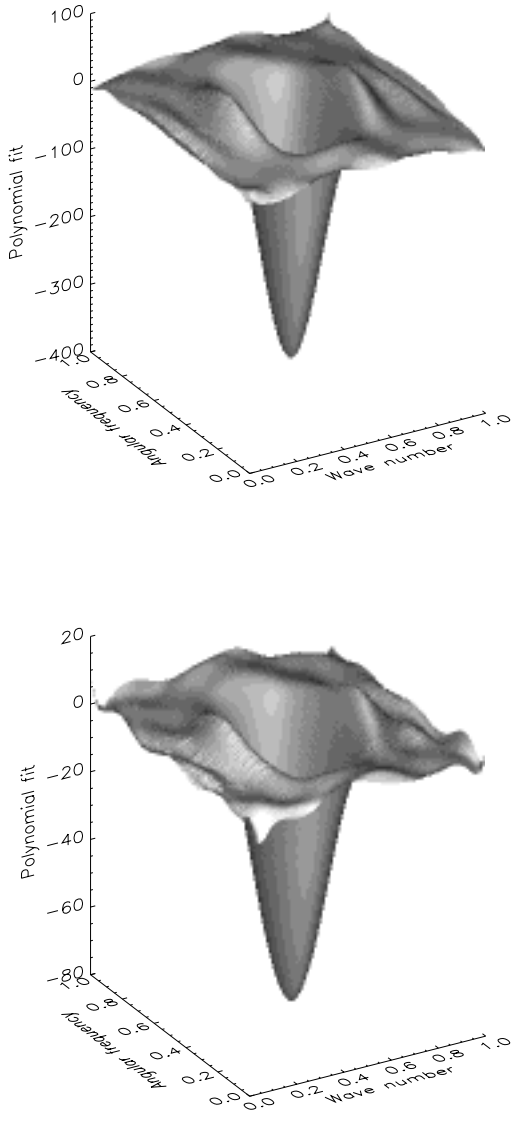

Fig. 4. Fits of the PCH artifact computed from the αCep (top) and PCyg (bottom) biased power spectra (coordinates are in arbitrary unit)

4.3. Application to visibility estimates

The visibilities obtained from the GI2T are determined by computing the ratio of high to low frequency energies in the power spectrum. In theory the support of the high-frequency components are defined by the AC of the output pupil of the GI2T. In practice, the geometry of this ouput pupil is subject to mis-alignment of the optics or telescopes guiding errors. Also, optical path difference variations spread the high frequency energy accross the wave number axis. Therefore, the high frequency support is not exactly known. Until now, we have used the

following criteria for determining the fringe support: the points close to the cut-off frequency being at the level of the photon noise, only the frequencies where the signal is twice as large as the photon noise were taken into account. Thus the visibility measurement is directly signal to noise dependent. With the present correction where the PCH is removed, the high frequency peak can be integrated on a support larger than its cut-off frequency without changing the total energy. This is due to the fact that points outside this peak have now a zero mean value.
Therefore, the estimate of the high frequency energy does not depend on the exact extent of its support anymore. However its signal to noise ratio is determined as the ratio between the high frequency energy and an energy defined as the integration of the standard deviation of the noise over a support corresponding to the high frequency peak. This support, that is not necessary for the visibility measurement itself, is determined by taking into account just the points exceedings twice the standard deviation of the noise. The uncertainty on a visibility measurement is defined as the following (M94b):

$$\mathrm{d}V = \frac{V}{2(S/N)}\left(1+\frac{V^2}{2}\right), \tag{6}$$

From Table 3, one sees that the effect of support variation in the wave number direction corresponds to visibility variations smaller than the error on the latter. The same result is obtained by growing the support in the angular frequency direction.

Table 3. Visibility variations versus support size. (In the wave number direction: 1 pixel corresponds to $1/\Delta\lambda$. In the angular frequency direction: 20 pixels correspond to D/λ. In our case, $\Delta\lambda = 7$ nm, $\lambda = 670$ nm, $D = 1.5$ m and $S/N = 13.8$)

support size (pixels)	Visibility (%)
15×50	72.1 ± 3.3
20×50	71.5 ± 3.2
25×50	72.2 ± 3.3
30×50	72.0 ± 3.3
35×50	72.0 ± 3.3
40×50	71.6 ± 3.3

4.4. Observation of αCep

In this paragraph, we demonstrate the improvement of visibility estimates with our technique over previous data reduction methods (M94b, Mourard et al. 1997). We use observations of αCep (night of October 16, 1994) in the spectral band 669 to 675 nm near the HeI line. The 30 minutes of observation are divided in sequences of 3 minutes. For each sequence, the power spectrum is obtained by Fourier transforming the averaged AC of the 20 ms frames recorded by the CP40. Each short exposure contains 120 photons on average. The power spectra are processed to remove the artifact due to the PCH. Thus, the visibilities are derived from the unbiased power spectra. The result is presented in Fig. 5. From the set of individual visibility measurements, we calculate a nightly average and a standard deviation $V = 64.7 \pm 1.8\%$. This standard deviation gives a good estimate for the error on the visibility. The same work has been carried out (Mourard et al. 1997) by using the old PCH correction method. The hole was filled in using polynomial interpolations along the central rows of the AC (in the direction of dispersion). The obtained nightly average and standard deviation were $V = 65.6 \pm 2.8\%$. So, the relative error on the visibility has been reduced by about 1/3 by using the new PCH correction.

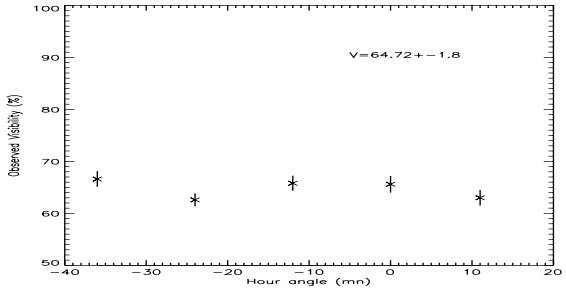

Fig. 5. Short-sequence visibility measurements for αCep on one night ($S/N = 14.0$)

5. Conclusion

We have studied the problem of the PCH in the GI2T data processing. This PCH appearing in the AC of fringe pattern is produced by the CP40 detector itself which can detect only 1 photon per pixel and per exposure time of 20 ms. We propose to remove the corresponding artifact in the power spectrum by fitting a 2D polynomial function to the Fourier transform of the PCH in order to reconstruct the original unbiased power spectrum. Among the a posteriori correction methods, it is certainly the easier and the most efficient one. Actually, the Hoffman method (Hoffman 1993) requires the PCH calibration on a laboratory source and the method, which consists in interpolating the PCH in the direct space, is less efficient because the hole has a narrow support at the center of the AC. Besides, in terms of the signal to noise ratio, the present a posteriori correction method is superior to CC techniques (Thiébaut 1994). We have also shown a significant improvement in visibility measurements due to the correction over previous GI2T data reduction (M94b). After the PCH removal, the visibility estimate becomes signal to noise

independent and more reliable. This has been demonstrated both on simulated and actual data from GI2T observations of αCep and PCyg.

However, all these improvements are strongly dependent on the fit accuracy. The PCH removal will be correct only if the signal support in the spectral density masks only a small part of the PCH Fourier transform. Consequently, the fringes must be oversampled with respect to the PCH size instead of the detector pixel. Therefore, provided a correct oversampling, this method can be applied to other imaging techniques.

Acknowledgements. We are grateful to E. Thiebaut and R. Foy for many useful discussions and to P. Stee for a critical review of the original manuscript. The GI2T is supported by the PNHRAA french organisation from CNRS-INSU.

References

Berio P., Mourard D., Vakili F., 1997, J. Opt. Soc. Am. 14, 1
Blazit A., 1987, PhD, Univ. of Nice
Dainty J.C., "Stellar speckle interferometry" in Speckle and Related Phenomena, Dainty J.C. (ed.) Vol. 9 of Topics in Applied Physics. Springer-Verlag, Berlin, 1975
Foy R., 1987, "Speckle Imaging Review", Proceedings of the Ninth Summer Workshop in Astronomy and Astrophysics on Instrumentation for Ground-based Optical astronomy, University of California, Santa Cruz, Robinson L.B. (ed.). Springer-Verlag, pp. 345-359
Fried D.L., 1965, J. Opt. Soc. Am. 55, 1427
Hoffman K.-H., 1993, J. Opt. Soc. Am. A 10, 2
Labeyrie A., 1970, A&A 6, 85
Mourard D., Tallon-Bosc I., Blazit A., et al., 1994a, A&A 283, 705
Mourard D., Tallon-Bosc I., Rigal F., et al., 1994b, A&A 288, 675
Mourard D., Bonneau D., Koechlin L., 1997, A&A 317, 789
Petrov R., Roddier F., Aime C., 1986, J. Opt. Soc. Am. 3, 5
Roddier F., Léna P., 1984, J. Opt. (Paris) 15, 4, 171-182
Thiébaut E., 1994, A&A 284, 340
Thiébaut E., Balega Y., Balega I., et al., 1995, A&A 284, 304, L17-L20
Weigelt G., 1977, Opt. Commun. 21, 55-59